Computers & Structures Vol. 33, No. 4, pp 1107–1115, 1989
Printed in Great Britain.

0045-7949/89 $3.00 + 0.00

FORCE AND MOMENT CORRECTIONS FOR THE WARPED FOUR-NODE QUADRILATERAL PLANE SHELL ELEMENT

B. P. NAGANARAYANA and G. PRATHAP
Structural Sciences Division, National Aeronautical Laboratories, Bangalore 560017, India

(*Received* 14 *November* 1988)

Abstract—A four-node quadrilateral plate element can be used as a facet shell element only if provision is made to allow for non-coplanarity of the four nodes. The element stiffnesses are generated for a 'mean plane' equidistant from the four nodes, and are corrected by introducing equilibrated forces and moments as the element is 'moved' to the original nodes. In this paper we introduce a rational procedure for determining the 'kick-off forces' and show that the procedure used in NASTRAN violates a virtual work condition and leads to difficulties in certain warped configurations.

1. INTRODUCTION

Because of their inefficient and inaccurate behaviour, triangular elements have been replaced by quadrilateral elements for most practical applications. In particular, the QUAD4 (four-noded linear quadrilateral shear flexible element) has gained pre-eminence in most plate and shell applications, because of its simplicity and reasonably high accuracy. The fundamental difficulties related to the field- and edge-consistencies have been successfully described and overcome [1].

Generally, the shell contours may be such that plane elements cannot be fitted in, i.e. the four nodes of the element will not be coplanar. In such situations, the facet (mean-plane) approximation of the shell structure may lead to highly inaccurate results, because of the incompatibility between the adjacent elements with non-unique connecting nodes during stiffness assembly. Hence, the element stiffness matrices should be transformed onto the actual element nodes before global assembly. Such transformation of the in-plane stiffnesses gives rise to moment inequilibrium about the local x- and y-axes. Because, in a general mesh, the adjacent elements may not always access moments (e.g. bar elements), it is necessary to counteract these inequilibrating moments by additional stiffness in the normal deflection d.o.f.

This has been achieved, to some extent, by satisfying the equilibrium conditions only on each edge and then superimposing the normal force components on the corresponding nodes [2, 3]. It should be noted that such a procedure is incomplete. This solution, using an edge-by-edge approach, was resorted to as there were only three equilibrium equations from which four unknown normal forces had to be determined.

In this work, the principle of virtual work has been used to construct the other equation required to solve the four unknowns over the element domain, rather than over the element boundary. As the additional 'normal' forces are 'fictitious', they should not disturb the energy of the system, i.e. the total 'virtual work' done by these forces, during the process of the transformation, should be zero.

In fact, the edge-by-edge satisfaction of equilibrium, adapted by the CSA*NASTRAN element, violates this condition for some configurations and fails to give correct answers in such cases.

2. ELEMENT FORMULATION

The mean plane is constructed using the mid-points of the four edges (Fig. 1). The vector product of **DB** and **AC** gives the local normal (z-direction). The local x-direction is fixed along **DB** and the local y-direction is fixed orthogonal to the other two directions.

If $\mathbf{x}_i$ and $\mathbf{X}_i$ are the position vectors of the point 'i' in the local and global coordinates respectively, we have

$$\mathbf{b}_1 = (\mathbf{X}_B - \mathbf{X}_D)$$

$$\mathbf{b}_3 = (\mathbf{X}_B - \mathbf{X}_D) * (\mathbf{X}_C - \mathbf{X}_A)$$

$$\mathbf{b}_2 = \mathbf{b}_3 * \mathbf{b}_1 .$$

Normalizing the vectors $\mathbf{b}_i$ to $\mathbf{a}_i$, we have the direction cosine matrix $[a]$, such that

$$\mathbf{X}_i = [a] * \mathbf{x}_i. \tag{1}$$

If $\{d^e\}$ and $\{D^e\}$ are the element nodal displacement vectors in local and global Cartesian coordinate systems, and $[T1]$ is the corresponding transformation matrix, we can write

$$\{d^e\} = [T1] * \{D^e\} \tag{2}$$

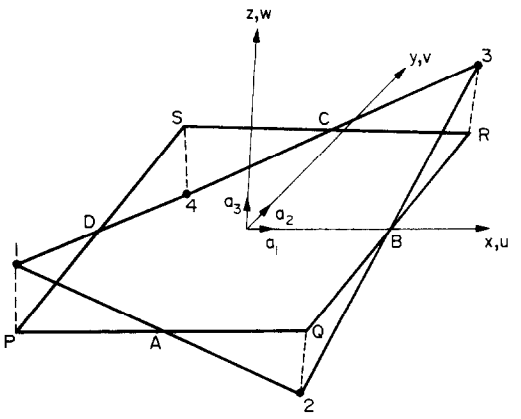

1 X, Y, Z - Global cartesian coordinates
U, V, W - Global cartesian displacements
$(-)_x, (-)_y, (-)_z$ - Global cartesian rotation
2 x, y, z - Local cartesian coordinates
u, v, w - Local cartesian displacements
$\theta_x, \theta_y, \theta_z$ - Local cartesian displacements

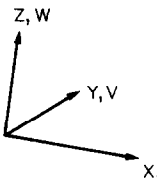

1-2-3-4 Actual element
P-Q-R-S Mean plane element
A, B, C, D Mid points

Fig. 1. The four-node warped plane shell element.

and

$$[K^e]_{\text{global}} = [T1]^T * [K^e]_{\text{local}} * [T1]. \tag{3}$$

2.1. Force correction based on equilibrium on edges [2, 3]

Let PQRS be the mean plane corresponding to the actual element 1234 (Fig. 1). Then nodes 1, 2, 3 and 4 will be 'H' units (say) above and below the mean plane alternatively. The forces in the x- and y-directions are resolved to the edge-parallel forces at each node 'i' as

$$\begin{Bmatrix} f_{i,i+1} \\ f_{i,i-1} \end{Bmatrix} = \frac{1}{\sin(\theta_i - \theta_{i-1})} \begin{bmatrix} -\sin\theta_i & \cos\theta_i \\ -\sin\theta_{i+1} & \cos\theta_{i+1} \end{bmatrix} \begin{Bmatrix} f_{xi} \\ f_{yi} \end{Bmatrix}, \tag{4}$$

where the suffices vary in cyclic manner. The angles and forces are shown in Fig. 2 with their directions.

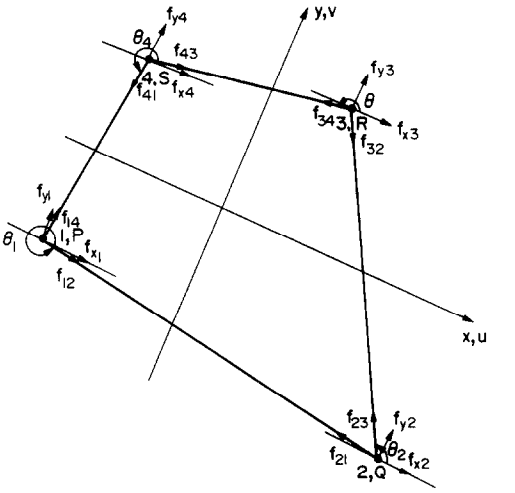

Fig. 2. Resolution of 'in-plane' forces into 'edge' forces [2, 3].

Considering the equilibrium on the edge PQ (Fig. 3), we obtain

$$f_{ZA} = (f_{12} + f_{21}) * (H/2L_{PQ}). \tag{5}$$

Superimposing the results from all the edges, we obtain

$$\{f\} = [T2]^T \{f'\}, \tag{6}$$

where

$$\{f\} = \{f_{x1}\, f_{y1}\, f_{z1}\, M_{x1}\, M_{y1} \ldots\}$$

$$\{f'\} = \{f_{xp}\, f_{yp}\, f_{zp}\, M_{xp}\, M_{yp} \ldots\}$$

are the nodal force vectors for the actual element and the mean plane (m.p.) respectively. The same transformation can also be used for the displacements, such that

$$[K^e]_{\text{local}} = [T2]^T * [K^e]_{\text{m.p.}} * [T2]. \tag{7}$$

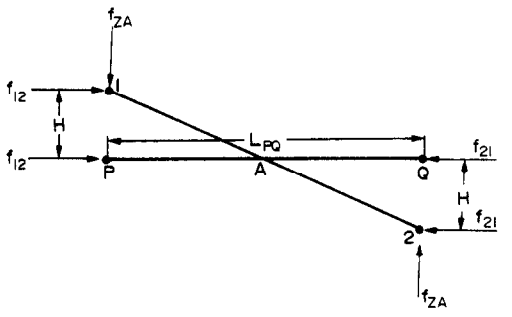

Fig. 3. Edge 1–2 under equilibrium during 'force' correction.

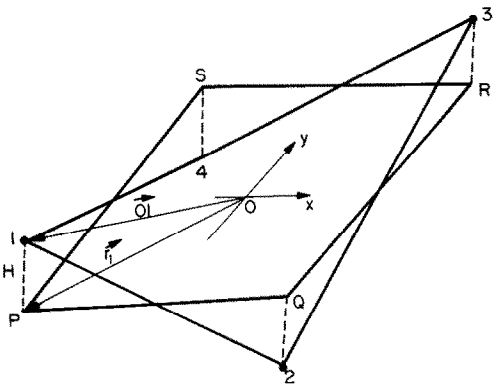

Fig. 4. Force correction based on equilibrium over the element domain and 'zero virtual work principle'.

2.2. Force correction based on equilibrium and virtual work principles

As is evident from Fig. 4, the moment equilibrium in the mean plane gives rise to

$$\sum_{i=1,4} (f_{xi}\mathbf{i} + f_{yi}\mathbf{j}) * \mathbf{r}_i = 0, \tag{8a}$$

where $\mathbf{r}_i$ are the position vectors of the mean plane nodes P to S, with respect to the local origin. Moment equilibrium for the real element leads to

$$\sum_{n=1,4} (f_{xn}\mathbf{i} + f_{yn}\mathbf{j} + f_{zn}\mathbf{k}) * \mathbf{On} = 0. \tag{8b}$$

On simplification, (8a) and (8b) give rise to the three moment equilibrium equations

$$\sum_{i=1,4} f_{yi}x_i = \sum_{i=1,4} f_{xi}y_{yi} \tag{9a}$$

$$\sum_{i=1,4} f_{zi}x_i = \sum_{i=1,4} f_{xi}z_i \tag{9b}$$

$$\sum_{i=1,4} f_{zi}y_i = \sum_{i=1,4} f_{yi}z_i \tag{9c}$$

and the force equilibrium in the three directions gives

$$\sum_{i=1,4} f_{xi} = 0 \tag{10a}$$

$$\sum_{i=1,4} f_{yi} = 0 \tag{10b}$$

$$\sum_{i=1,4} f_{zi} = 0. \tag{10c}$$

We have now three equations, (9b), (9c) and (10c), to solve for f_{zi} $(i = 1, 4)$ and hence the solution is 'indeterminate'. The fourth equation that is required can now be formed using the energy principles, i.e. the total virtual work done by the transformation of the 'normal' forces from the mean plane to the actual nodes should be zero, so as not to alter the total energy of the system, or

$$\sum_{i=1,4} f_{zi}z_i = 0. \tag{11}$$

By solving for the normal forces $f_{zi}(i = 1, 4)$ at the element nodes, using (9b), (9c), (10c) and (11), the 'variationally correct' $[T2]$ can be formed for the transformation of the 'forces' and consequently 'stiffnesses' from the mean plane of the element to the real element nodes as in eqns (6) and (7).

2.3. Moment correction

Shifting of the moments about the mean plane x- and y- axes, M_x and M_y, onto the real nodes does not disturb the equilibrium, but results in an unrealistic moment vector for the warped element. The moment about the normal to the actual surface should be zero, at each node. This can be achieved by adding a small moment component M_{zi} about the normal to the mean plane, at each node 'i', such that

$$(M_{xi}\mathbf{i} + M_{yi}\mathbf{j} + \mathbf{M}_{zi}\,\mathbf{k}) \cdot \mathbf{n}_i = 0, \tag{12}$$

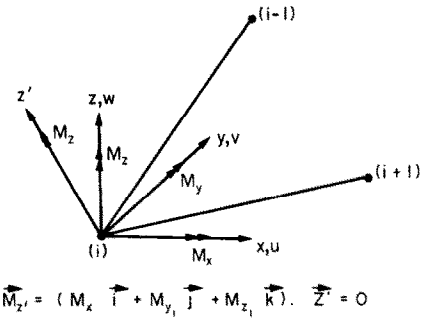

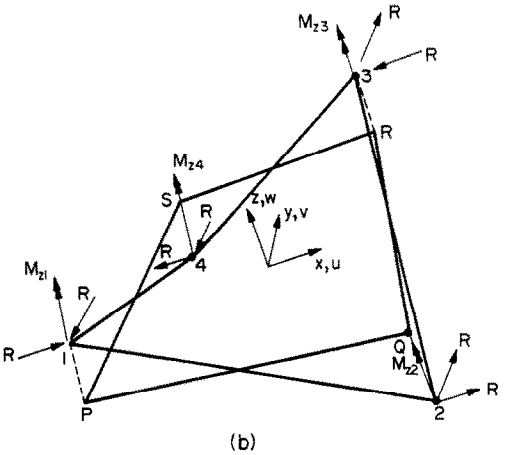

Fig. 5. Moment correction.

where $\mathbf{n}_i$ is the normal vector to the actual surface at node i. These additional moment components, M_{ti}, are then balanced by adding a system of self-equilibrating forces of equal magnitude R at each node in the x- and y-directions as shown in Fig. 5, such that

$$\sum_{i=1,4} (f_{xi}\mathbf{i} + f_{yi}\mathbf{j}) * \mathbf{r}_i + \sum_{i=1,4} M_{zi}\mathbf{k} = 0. \quad (13)$$

Using (12) and (13) for the moment correction and the 'variationally correct' force correction derived earlier (Sec. 2.2), the final transformation matrix $[T2]$ can be formed such that

$$[K^e]_{\text{global}} = [T2]^T [T1]^T [K^e]_{\text{m.p}} [T1][T2]. \quad (14)$$

Note that if $[T2]$ is derived from Secs 2.1 and 2.3 instead, we obtain the CSA*NASTRAN element.

3. VIOLATION OF THE VIRTUAL WORK PRINCIPLE BY CSA*NASTRAN

If we consider only equilibrium conditions as the criteria, as in NASTRAN, and solve the 'indeterminate' system of equations on the element boundary, the total virtual work done by transforming the forces from the mean-plane nodes to the actual nodes may be non-zero for certain load cases. For example, consider the load case 1 of Fig. 6. The edges 1–2 and 4–3 are under the loads of equal magnitude f as shown in the figure. According to the NASTRAN

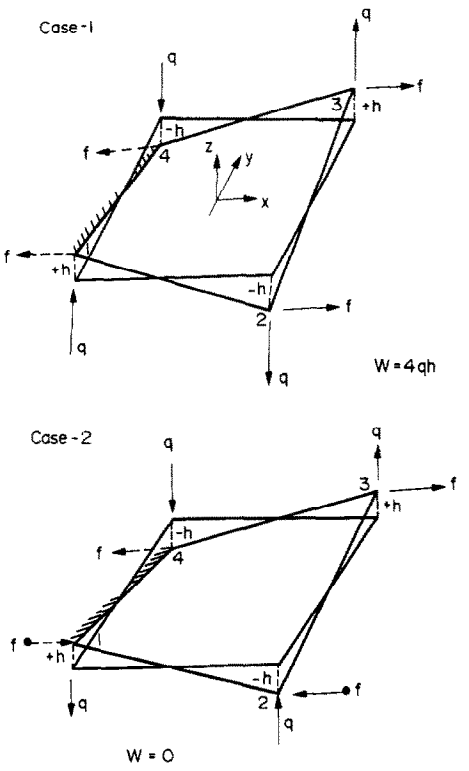

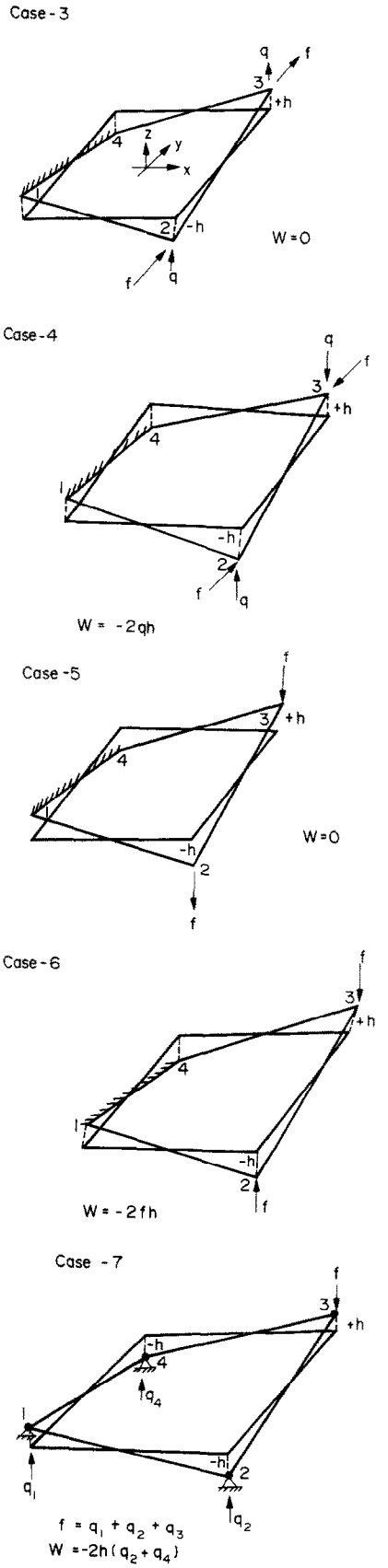

Fig. 6. Single element tests—failure of NASTRAN element for load cases 1, 4, 6 and 7 (example 4.1).

procedure [2, 3], the moment equilibrium of these two edges requires inclusion of the forces of magnitude q normal to the mean plane as shown, such that

$$q = 2*f*h/L, \tag{15}$$

where L is the side length of the 'square' mean plane and h is the warping height. Hence, for the load case 1, the total work done by the transformation of the forces onto the real nodes from the mean plane is

$$W = \sum_{i=1,4} (\mathbf{p}_{xi} \cdot \mathbf{s}_{xi} + \mathbf{p}_{yi} \cdot \mathbf{s}_{yi} + \mathbf{p}_{zi} \cdot \mathbf{s}_{zi})$$

$$= \sum_{i=1,4} (\mathbf{p}_{zi} \cdot \mathbf{s}_{zi})$$

$$= 4*(q \cdot h), \tag{16}$$

where **p** and **s** stand for the force and displacement vectors. Similarly, it can be proved that the total virtual work done by the 'force transformation' is non-zero for load cases 4, 6 and 7, if the edge-wise equilibrium satisfaction is done as in NASTRAN, thus violating the fourth condition that is derived from the principle of virtual work.

4. NUMERICAL EXAMPLES

The numerical examples are chosen so as to concentrate attention on the behaviour of the QUAD4 when it is 'warped'. The following versions of QUAD4 are used for the comparative study:

Q4-0	Mean-plane stiffness is given a force correction based on the equilibrium conditions and the zero virtual work condition.
Q4-1	Q4-0 + moment correction.
NASTRAN	QUAD4 in CSA*NASTRAN-V87B (force correction based on equilibrium on the element boundary plus moment correction).

4.1. Single element tests

A single element, with square and horizontal mean plane, is tested for the following load cases:

(1) In-plane stretching (Table 1),
(2) In-plane couple (about the z-axis) (Table 2),
(3) In-plane shear bending (Table 3),
(4) In-plane pinching loads (Table 4),
(5) Out-of-plane shear bending (Table 5),
(6) Out-of-plane couple (about the x-axis) (Table 6), and
(7) Constant twisting moment test (Table 7),

Table 1. In-plane stretching [Fig. 6(1)]: example 4.1

Element	$h = 0.0$	$h = 0.1$	$h = 1.0$
(A) U-Displacements at nodes 3 and 4 ($t = 0.1$)			
Q4 – 0	0.9758713 – 05	0.9906581 – 05	0.9998485 – 05
Q4 – 1	0.9758713 – 05	0.9906581 – 05	0.9998485 – 05
NASTRAN	0.9758713 – 05	0.6880395 – 04	0.5914285 – 02
(B) W-Displacements at nodes 3 and 4 ($t = 0.1$)			
Q4 – 0	0.0	−0.9192455 – 04	−0.1490583 – 04
Q4 – 1	0.0	−0.9192455 – 04	−0.1490583 – 04
NASTRAN	0.0	−0.2952205 – 02	−0.2902125 – 01

Table 2. In-plane couple loading [Fig. 6(2)]: example 4.1

Element	$h = 0.0$	$h = 0.1$	$h = 1.0$
(A) U-Displacements at nodes 3 and 4 ($t = 0.1$)			
Q4 – 0	0.273 – 04	0.1437369 – 03	0.1167099 – 01
Q4 – 1	0.273 – 04	0.1436333 – 03	0.1086815 – 01
NASTRAN	0.273 – 04	0.1436354 – 03	0.1086834 – 01
(B) W-Displacements at nodes 3 and 4 ($t = 0.1$)			
Q4 – 0	0.0	0.5821844 – 02	0.5821844 – 01
Q4 – 1	0.0	0.5817159 – 02	0.5420904 – 01
NASTRAN	0.0	0.5817263 – 02	0.5421001 – 01

Table 3. In-plane shear bending [Fig. 6(3)]: example 4.1

Element	$h = 0.0$	$h = 0.1$	$h = 1.0$
(A) V-Displacements at nodes 3 and 4 ($t = 0.1$)			
Q4 – 0	0.533 – 04	0.1697369 – 03	0.1169699 – 01
Q4 – 1	0.533 – 04	0.1696240 – 03	0.1089323 – 01
NASTRAN	0.533 – 04	0.1696261 – 03	0.1089342 – 01
(B) W-Displacements at nodes 3 and 4 ($t = 0.1$)			
Q4 – 0	0.0	0.5821844 – 02	0.5821844 – 01
Q4 – 1	0.0	0.5816925 – 02	0.5420675 – 01
NASTRAN	0.0	0.5817029 – 02	0.5420772 – 01

Table 4. In-plane pinching loads [Fig. 6(4)]: example 4.1

Element	$h = 0.0$	$h = 0.1$	$h = 1.0$
(A) V-Displacements at nodes 3 and 4 ($t = 0.1$)			
Q4 – 0	0.731903 – 05	0.8962012 – 05	0.9983169 – 05
Q4 – 1	0.731903 – 05	0.8962012 – 05	0.9983169 – 05
NASTRAN	0.731903 – 05	0.6635979 – 04	0.1611397 – 02
(B) W-Displacements at nodes 3 and 4 ($t = 0.1$)			
Q4 – 0	0.0	−0.3064152 – 03	−0.4968610 – 04
Q4 – 1	0.0	−0.3064152 – 03	−0.4968610 – 04
NASTRAN	0.0	−0.2952092 – 02	−0.2952093 – 01

Table 5. Out-of-plane shear bending [Fig. 6(5)]: example 4.1

Element	$h = 0.0$	$h = 0.1$	$h = 1.0$
(A) W-Displacements at nodes 3 and 4 ($t = 0.1$)			
Q4 – 0	0.2910922 + 00	0.2910922 + 00	0.2910922 + 00
Q4 – 1	0.2910922 + 00	0.2908825 + 00	0.2710692 + 00
NASTRAN	0.2910974 + 00	0.2908877 + 00	0.2710741 + 00
(B) U-Displacements at nodes 3 and 4 ($t = 0.1$)			
Q4 – 0	0.0	0.5821844 – 02	0.5821844 – 01
Q4 – 1	0.0	0.5816925 – 02	0.5420675 – 01
NASTRAN	0.0	0.5817029 – 02	0.5420772 – 01

Table 6. Out-of-plane couple [Fig. 6(6)]: example 4.1

Element	$h = 0.0$	$h = 0.1$	$h = 1.0$
(A) W-Displacements at nodes 3 and 4 ($t = 0.1$)			
Q4 – 0	0.1476005 + 00	0.5714643 – 01	0.9258700 – 03
Q4 – 1	0.1476005 + 00	0.5714643 – 01	0.9266457 – 03
NASTRAN	0.1476071 + 00	0.1476071 + 00	0.147607 + 00
(B) V-Displacements at nodes 3 and 4 ($t = 0.1$)			
Q4 – 0	0.0	−0.3064152 – 03	−0.4968610 – 04
Q4 – 1	0.0	−0.3064152 – 03	−0.4968610 – 04
NASTRAN	0.0	−0.2952092 – 02	−0.2952093 – 01

Table 7. Constant twisting moment [Fig. 6(7)]: example 4.1

Element	$h = 0.0$	$h = 0.1$	$h = 1.0$
(A) W-Displacement at node 4 ($t = 0.1$)			
Q4 – 0	0.7144286 + 00	0.1211114 + 00	0.1455363 – 02
Q4 – 1	0.7144286 + 00	0.1211114 + 00	0.1455363 – 02
NASTRAN	0.7144571 + 00	0.7598978 – 01	0.8493293 – 03
(B) U/V-Displacement at node 4 ($t = 0.1$)			
Q4 – 0	0.0	−0.3460325 – 03	−0.4158179 – 04
Q4 – 1	0.0	−0.3460325 – 03	−0.4158179 – 04
NASTRAN	0.0	−0.1063857 – 02	−0.1189061 – 04

for varying degrees of warping. The dimensions are $L = 10$, $b = 10$ and warping heights $h = 0.0, 0.1, 1.0$; the elastic properties are Young's modulus = 1.0E + 06 and Poisson's ratio = 0.3.

From Sec. 3. and Fig. 6, it is very clear that the NASTRAN element violates the zero virtual work condition in load cases 1, 4, 6 and 7. Hence the NASTRAN version of QUAD4 is expected to fail in these load cases. Tables 1, 4, 6 and 7 confirm this. In fact, the error increases exponentially with the warping height h (Fig. 7).

Careful observation of the results show that, in the cases where CSA*NASTRAN fails, the moment correction has no influence on the results. Hence it can be concluded that *the 'zero virtual work condition' is an essential condition in addition to the equilibrium conditions*, and gives corrections to the stiffnesses related to the local normal displacements.

The same tests were repeated with a 'distorted' mean plane. The results were qualitatively the same as above and the parasitic shear locking was completely removed when 'field-consistent' global derivatives were used in defining the in-plane shear strain field. The results are not tabulated.

4.2. Spherical cap

A doubly curved shallow shell of spherical contour of radius 96 units and a square base of edge length 32 units with diaphragm boundary conditions under a point load of 100 units normal to the shell surface at the centroid of the cap (Fig. 8) is considered. The analysis is done by modelling the third quarter of the

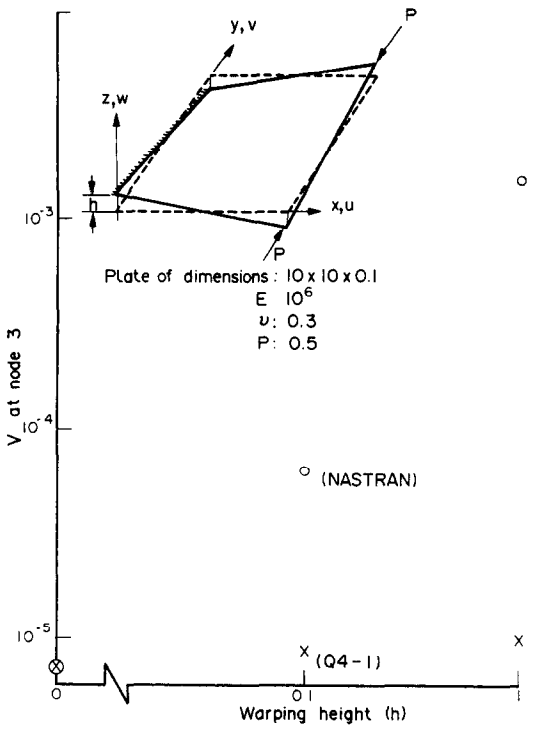

Fig. 7. Single element test—pinching loads at the tip. Pinching displacements for different warping heights (example 4.1, load case 4).

cap with a 6*6 finite element mesh. The material used has Young's modulus = 0.1E + 08 and Poisson's ratio = 0.3. Table 8 compares the maximum normal displacement at the centroid, obtained from Q4-1, with the CSA*NASTRAN element for different thicknesses. As the warping in this case is negligible, both element versions give correct answers.

4.3. *Hemispherical shell*

Here, a hemisphere of radius 10 units, truncated at 18° from the axis of the shell, is subjected to four unit point loads normal to its base rim alternating in sign at intervals of 90° (Fig. 9). The material has Young's modulus = 0.6825E + 08 and Poisson's ratio = 0.3. Because of symmetry in geometry as well as loading, a quadrant is considered for analysis with an 8*8 element mesh. Both membrane and bending strains contribute significantly to the radial displacements at the load points. A comparison of the results (the deflection under the pinching load) is presented in Table 9 for varying thickness t. As the warping of elements in this case is negligible, both Q4-1 and NASTRAN pass this test.

4.4. *Twisted beam*

Here we consider a practical problem which throws light on the warping effects, as the structure considered is highly warped over its length. A twisted rectangular strip of material of Young's modulus of 0.29E + 08 and Poisson's ratio of 0.22 with geometric dimensions of length = 12.0, width = 1.1, twist (root-to-tip) = 90° and thickness = 0.32, 0.16, 0.08, is clamped at one end and is subjected to a unit in-plane load ($F_z = 1.0$) at the other end (Fig. 10). A 12*2 finite element mesh is used.

Table 10(a) presents the comparative results (the displacements at the free tip in the load direction) from Q4-0, Q4-1 and NASTRAN. The element without warping corrections 'locks' severely in this case. But, as in load case (3) of test example 4.1, there is no violation of the zero virtual work condition. Hence NASTRAN passes this test. Table 10(a) presents the tip displacements under the load for varying thickness, showing very close behaviour of Q4-1 and NASTRAN.

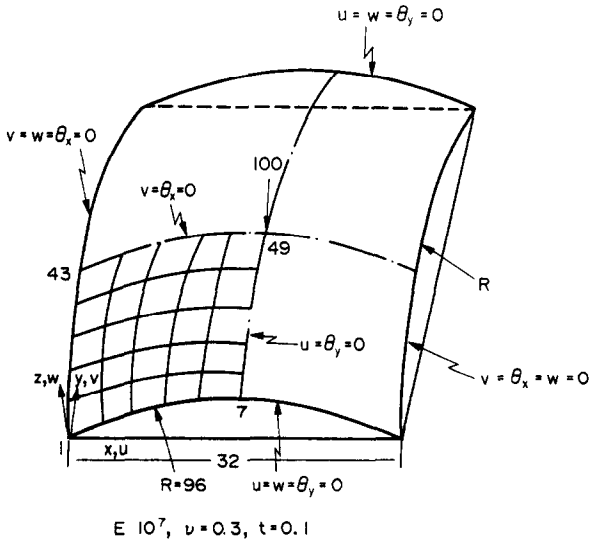

E 10^7, υ = 0.3, t = 0.1

Fig. 8. Spherical cap (example 4.2).

Table 8. Spherical cap (Fig. 8): example 4.2; 'normal' deflection under the central load

Element	$t = 0.1$	$t = 0.01$	$t = 0.001$
Q4 – I	0.3257 – 01	0.1214 + 01	0.1665 + 02
NASTRAN	0.3256 – 01	0.1209 + 01	0.1662 + 02

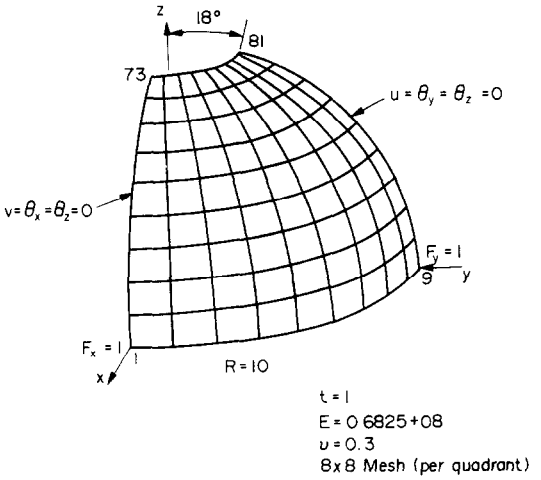

Fig. 9. Pinched hemisphere (example 4.3).

Table 10(b) shows the free tip displacements in the load direction when the load is tensile along the axial direction ($F_x = 1.0$). As expected, because the zero virtual work condition is violated, CSA*NASTRAN fails this test; the behaviour is similar to load case (1) of numerical experiments 4.1. The results are graphically represented in Fig. 10. It can be seen that the 'thickness' has a relatively negligible influence on results when compared with 'warping height'. The failure will be more distinct and critical with higher degrees of warping (i.e. coarser mesh). It can be noted that the moment correction has a negligible influence on the results, as in its counterpart load case in the single element tests.

5. CONCLUSIONS

We have developed here a four-noded shear flexible plane shell element which can take care of both the 'distortion' and 'warping' requirements that arise because of the complexity of the shell structure. We have demonstrated how the virtual work principle plays a very important role in addition to equilibrium conditions in determining the 'force corrections' from the mean plane to the real position. It has been proved that the NASTRAN element violates the condition of zero total virtual work done by the 'normal forces', which are added to balance the moments produced during the transformation of the in-plane forces from the mean plane to the non-coplanar nodes of the element, in several 'single element' tests. Several numerical experiments (Sec. 4.1) have confirmed the failure of the NASTRAN QUAD4 in the corresponding test cases. The correction to the element stiffnesses related the in-plane displacements and the mean plane 'normal' rotation, so that the moment about the normal to the actual surface at each node, as well as the moment about the normal to the element mean plane over the element domain after transforming the forces and moments from the mean plane to the actual nodes, will vanish. It is also observed, in all the test cases where NASTRAN fails, that the moment correction has no influence on the element behaviour. Hence we conclude that the principle of virtual work poses an essential condition to be satisfied apart from the equilibrium conditions, if the warping correction has to be rational.

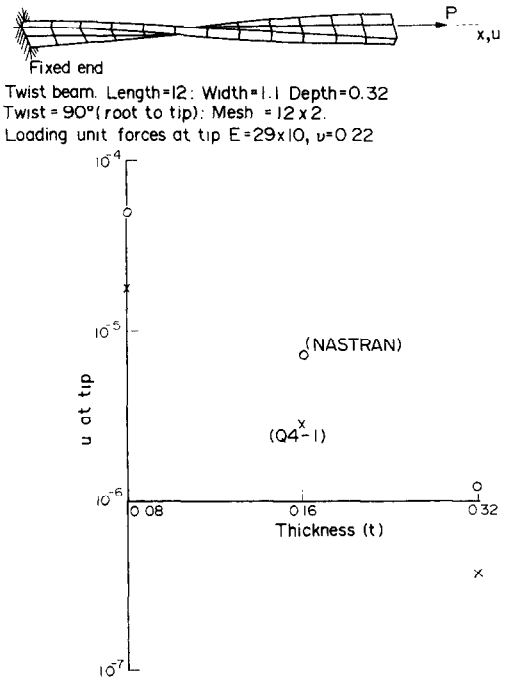

Fig. 10. Twisted beam under tip loads. Displacements under the stretching load for varying thickness (example 4.4).

Table 9. Pinched hemisphere (Fig. 9): example 4.3; displacements under pinching loads

Element	$t = 0.1$	$t = 0.01$	$t = 0.001$
Q4 – I	0.8548 – 04	0.7560 – 01	0.7545 + 02
NASTRAN	0.8558 – 04	0.7560 – 01	0.7546 + 02

Table 10. Twisted beam (Fig. 9): example 4.4

Element	$t = 0.32$	$t = 0.16$	$t = 0.08$
(a) Tip W-deflection under in-plane shear load ($F_z = 1.0$)			
Q4 – 0	0.5923 + 00	0.2807 + 01	0.1215 + 02
Q4 – 1	0.5268 – 02	0.4143 – 01	0.3290 + 00
NASTRAN	0.5277 – 02	0.4153 – 01	0.3307 + 00
(b) Tip displacements under the stretching load ($F_x = 1.0$)			
V-Displacements			
Q4 – 0	0.1167 – 05	0.2373 – 05	0.4976 – 05
Q4 – 1	0.1167 – 05	0.2373 – 05	0.4978 – 05
NASTRAN	0.1205 – 05	0.2594 – 05	0.6464 – 05
U-Displacements			
Q4 – 0	0.3714 – 06	0.2824 – 05	0.1812 – 04
Q4 – 1	0.3788 – 06	0.2863 – 05	0.1825 – 04
NASTRAN	0.1231 – 05	0.7497 – 05	0.5013 – 04
W-Displacements			
Q4 – 0	0.1334 – 07	0.5222 – 07	0.2855 – 06
Q4 – 1	0.1350 – 07	0.5288 – 07	0.2879 – 06
NASTRAN	0.6117 – 08	0.1595 – 07	0.4031 – 07

Acknowledgements—The authors are deeply indebted to Prof. R. Narasimha, Director, and Dr. K. N. Raju, Head, Structures Division, National Aeronautical Laboratories, Bangalore, for their constant encouragement and keen interest in the subject. The authors are also grateful to Mr. B. S. Madhusudan, Scientist, Structures Division, N.A.L., for some useful discussions.

REFERENCES

1. G. Prathap and B. R. Somashekhar, Field and edge consistency synthesis of a 4-noded quadrilateral plate bending element. *Int. J. Numer. Meth. Engng* **26,** 1693–1708 (1988).
2. R. D. Cook, *Concepts and Applications of Finite Element Analysis*, 3rd Edn. John Wiley, New York (1981).
3. R. H. MacNeal, *The NASTRAN Theoretical Manual* (1972).